DOI: 10.1002/adma.200700627

# Fiber Shaped Organic Light Emitting Device**

By *Brendan O'Connor*, *Kwang H. An*, *Yiying Zhao*, *Kevin P. Pipe*, and *Max Shtein**

Advances in fiber and fabric technology have been applied in a wide variety of contexts, ranging from structural composites to fiber-optic communications, and more recently, electronic textiles.[1–3] There is growing interest in optoelectronic devices having a fiber form factor, including pulled fiber photodetectors,[4] optically pumped surface emitting fiber lasers,[5] photoluminescent polymer-coated fibers,[6,7] fiber-based Grätzel[8] and thin film semiconductor[9] solar cells, as well as organic light emitting devices (OLEDs) on a fiber.[10] Fiber-based OLEDs in particular have wide ranging applications from fabric integrated light sources to low cost solid-state lighting. However, there is a relative dearth of scientific literature providing a sound physical understanding of the impact that the fiber geometry has on device performance, or the challenges facing the realization of fiber-based and fabric-integrated optoelectronics.

In this work we focus on molecular organic compounds as the active device layers due to their inherent mechanical flexibility and compatibility with low cost device fabrication techniques.[11,12] Using these materials, we demonstrate a fiber-based OLED and analyze the physical effects that arise due to the non-planar device geometry. The thickness of the active layers in these devices is approximately 100 nm, orders of magnitude thinner than the typical fiber diameter (e.g. 50–1,000 μm), suggesting that energy conversion functionality can be incorporated into an individual fiber without affecting its mechanical characteristics. Additionally, as will be analyzed below, the electroluminescence spectrum is measured to be independent of the observation angle, which is in contrast to planar OLED geometries.

An archetypal OLED structure is considered,[13] as illustrated in Figure 1a, and applied to the fiber geometry, Figure 1b. The OLED consists of organic charge transport and emission layers sandwiched between a metallic anode and cathode. For the fiber-based device the layers were deposited conformally onto a 480 μm thick polyimide-coated silica fiber using vacuum thermal evaporation at $10^{-6}$ Torr; the cathode was deposited through a shadow mask. (Please refer to the Experimental Sec. for details on device growths.) Figure 1c shows a photograph of a 1 mm segment of the OLED formed concentrically around the fiber, emitting characteristic green light under forward electrical bias. Light emission in this device occurs through the semitransparent outer electrode. For a direct comparison of optoelectronic performance, a similar OLED structure was deposited on planar silicon and polyimide substrates, as will be discussed below.

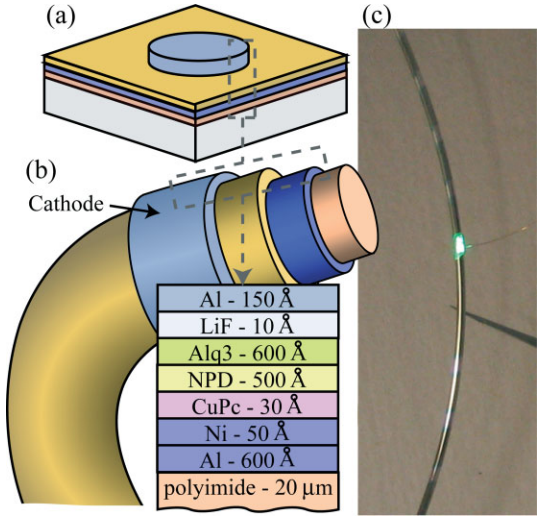


**Figure 1.** a) An illustration of a typical organic light emitting device (OLED) structure, along with b) an illustration of a fiber-based OLED structure analyzed in this report. c) A photograph of a flexed fiber having a 1 mm green light emitting "pixel" turned on.

Figure 2 compares the current density-voltage (*J–V*) characteristics of fiber OLEDs to those of the analogous planar devices. The similarity in the current-voltage relationship between the planar and fiber cells suggests comparable layer thickness of the hole and electron transport layers on each type of substrate.[14,15] The slightly larger leakage current at low bias (< 2.5 V) in one of the fiber-based devices is attributable to the greater surface roughness of the fiber substrate.

While the electrical characteristics do not differ materially between the fiber- and the planar-shaped OLEDs, their emission characteristics are expected to differ substantially due to the microcavity effects typical of OLEDs. Specifically, the microcavity effects present in the planar device structure lead to a strong variation in the peak wavelength with emission an-

[*] Prof. M. Shtein, Y. Zhao
Department of Materials Science and Engineering, University of Michigan
Ann Arbor, MI 48109 (USA)
E-mail: mshtein@umich.edu
B. O'Connor, K. H. An, Prof. K. P. Pipe
Department of Mechanical Engineering, University of Michigan
Ann Arbor, MI 48109 (USA)

[**] We thank Prof. Green's research group at the University of Michigan for their assistance with this work, the Office of Naval Research Contract No. N00014-05-0713, the National Science Foundation ECS-0523986, and the Air Force Office of Scientific research Contract No. FA9550-06-1-0399 for the financial support of this work.

ADVANCED MATERIALS

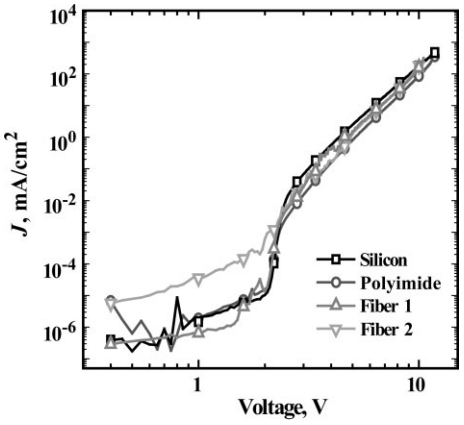


**Figure 2.** Current density–voltage (*J–V*) characteristics of the fiber and planar OLEDs. The planar OLEDs were deposited on silicon and polyimide substrates. The similar behavior between devices suggests comparable organic layer thicknesses. One of the fiber devices exhibits increased leakage current, attributed to substrate surface roughness leading to increased current shunt pathways.

gle.[16,17] Figure 3a and b show the electroluminescence (EL) spectra of the planar devices on silicon and polyimide substrates for different observation angles. The peak of the emission is shifted by as much as 40 nm on going from the normal to the in-plane observation angles. In contrast to the planar devices, as Figure 3c and d show, the fiber OLED exhibits an emission spectrum that is invariant with viewing direction. The origin of this behavior can be understood in terms of combined emission from a continuum of small planar OLEDs positioned around the circumference of the fiber. Indeed, as Figure 4 shows, the full width half maximum (FWHM) of the EL peak is invariant with angle for the fiber OLED, but is larger than the FWHM for the planar OLEDs over the majority of observation angles.

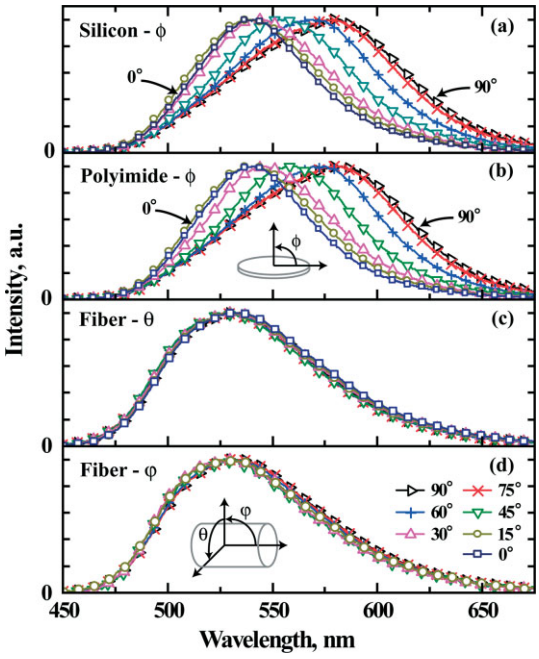


**Figure 3.** Emission spectrum with variation in observed angle for a) planar top-emitting OLED on silicon substrate; b) planar top-emitting OLED on polyimide substrate; c) fiber OLED with variation in azimuthal angle $\theta$; and d) fiber with variation in zenith angle $\varphi$. Normal emission is taken as 90° and the inset schematics illustrate the direction of angular variation. It is shown that the spectral character of the fiber is invariant to observation angle in contrast to the strong angular dependence observed in the planar devices.

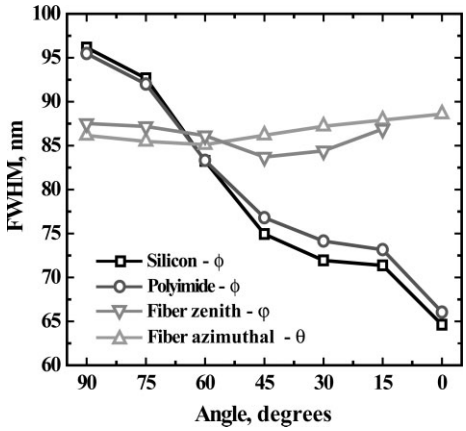


**Figure 4.** The spectral full width half maximum (FWHM) for the planar and fiber devices with variation in observed angle. The observation angle for each device is defined in Figure 3. The planar OLEDs show similar and strong variation in FWHM, while the fiber devices show invariant angular behavior.

Figure 5 compares experimental and predicted integrated emission intensity versus angle, where the model considers radiation from an isotropic distribution of oscillating dipoles confined within a microcavity.[18] The experiment and theory match well, with small deviations at off-normal emission angles attributable to increased scattering by surface imperfections. For comparison, a purely Lambertian emission pattern is also shown in Figure 5. Based on this light emissive behavior, and considering all directions of emission from the fiber and planar devices, the corresponding external quantum effi-

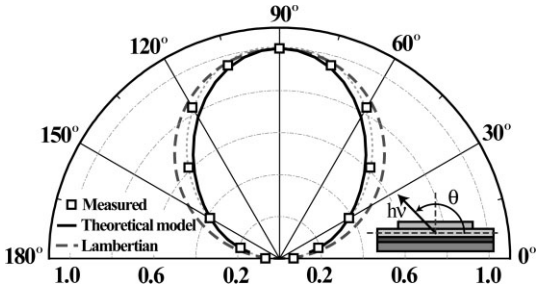


**Figure 5.** Electroluminescent intensity versus emission angle for a planar OLED with the device structure in Figure 1a. The experimental data is compared with a theoretical model of radiant power efficiency of dipole emission in the microcavity and a lambertian emission pattern.

ciency ($\eta_{EQE}$) versus current density is shown in Figure 6.[19] The efficiency of the "Fiber 1" device approaches that of the planar devices, with the difference attributable to minute vari-

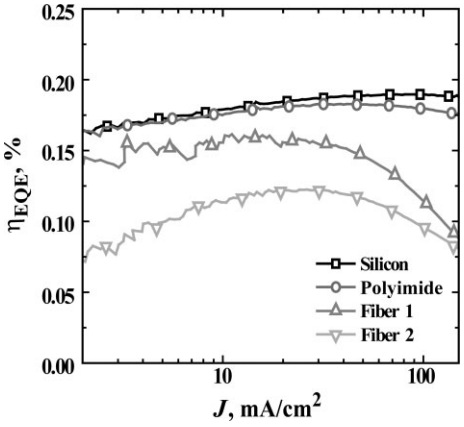


**Figure 6.** External quantum efficiency ($\eta_{EQE}$) for the planar and fiber OLED devices. These efficiency measurements correspond to the *J–V* curves of Figure 2.

ations in the anode and cathode thickness and roughness,[20] both of which can depend on the sticking coefficient of the adatoms, which in turn depends on the angle of arrival at the substrate.

The findings described above identify physical properties unique to the fiber geometry, with the potential for a wide range of applications (e.g., solid state lighting). We note, however, that the fiber geometry also presents unique challenges for processing, including, for example, the challenge of encapsulation for prolonged operational lifetime. It is anticipated, however, that the recent developments in the techniques for monolithic encapsulation of flexible OLEDs using parylene[21,22] and multilayer coatings[23,24] such as Barix™[25] are highly compatible with the fiber geometry and fabrication technique.

In summary, a considerable amount of research has emerged dealing with the EL spectral behavior of OLEDs,[16,26–30] specifically the microcavity effects that lead to variation in the emission spectrum with angle.[18,31–34] Additionally, there has been growing interest in non-planar device geometries for device applications.[1,35] In this study, we demonstrated OLEDs having a fiber for factor. We also experimentally and theoretically analyzed in detail some of the unique optoelectronic properties of these devices. The fiber OLED exhibits electrical characteristics and luminescence efficiency comparable to those of planar analogues, but at the same time offers a novel and promising device geometry with angularly uniform emission intensity across the entire emission spectrum. This property of fiber-based OLEDs is potentially of interest for display and lighting applications, as well as novel devices for application in fiber-optic communications and optical microscopy.

## *Experimental*

*OLED Fabrication*: The fiber substrate is a 480 μm thick polyimide-coated silica fiber. The planar and fiber-based OLEDs were grown by vacuum thermal evaporation at $10^{-6}$ Torr. For both planar and fiber substrates the deposition sequence was: aluminum, nickel, copper phthalocyanine (CuPc), *N,N′*-di-1-naphthyl-*N,N′*-diphenyl-1,1′-biphenyl-4,4′diamine (*α*-NPD), tris(8-hydroxyquinoline) aluminum ($Alq_3$), lithium fluoride (LiF) and aluminum. All layers were grown at rates of 2–3 Å $s^{-1}$, except for LiF and Ni layers, which were grown at 0.2 Å $s^{-1}$ with each layer thickness given in Figure 1. The nickel anode was oxidized prior to the deposition of the organic layers to facilitate hole injection, as described elsewhere [36,37]; the cathode was deposited through a shadow-mask [38]. The fiber substrate was axially rotated at a speed of 30 rpm during material deposition. The planar and fiber devices were cleaned according to a procedure described elsewhere [39].

*Device Characterization*: Devices on silicon and polyimide were grown simultaneously and characterized in close succession in the ambient. Devices on fibers were grown and tested separately, due to the difference in the deposition geometry. Device electrical characteristics were measured with an Agilent HP4156B semiconductor parameter analyzer. Optical intensity was measured with a Newport 818-SL power meter. Spectra were recorded using a fiber-coupled Ocean Optics USB2000-FL spectrometer and a collimating optical lens.

Received: March 15, 2007
Revised: June 2, 2007

[1] A. F. Abouraddy, M. Bayindir, G. Benoit, S. D. Hart, K. Kuriki, N. Orf, O. Shapira, F. Sorin, B. Temelkuran, Y. Fink, *Nat. Mater.* **2007**, *6*, 336.
[2] M. Hamedi, R. Forchheimer, O. Inganas, *Nat. Mater.* **2007**, *6*, 357.
[3] D. Marculescu, R. Marculescu, N. H. Zamora, P. Stanley-Marbell, P. K. Khosla, S. Park, S. Jayaraman, S. Jung, C. Lauterbach, W. Weber, T. Kirstein, D. Cottet, J. Grzyb, G. Troster, M. Jones, T. Martin, Z. Nakad, *Proc. IEEE* **2003**, *91*, 1995.
[4] M. Bayindir, F. Sorin, A. F. Abouraddy, J. Viens, S. D. Hart, J. D. Joannopoulos, Y. Fink, *Nature* **2004**, *431*, 826.
[5] O. Shapira, K. Kuriki, N. D. Orf, A. F. Abouraddy, G. Benoit, J. F. Viens, A. Rodriguez, M. Ibanescu, J. D. Joannopoulos, Y. Fink, M. M. Brewster, *Opt. Express* **2006**, *14*, 3929.
[6] S. S. Hardaker, R. V. Gregory, *MRS Bull.* **2003**, *28*, 564.
[7] K. L. Yi Yang, S. H. Na, S. Yin, Q. Wang, in *Light-Emitting Diodes: Research, Manufacturing, and Applications IX*, Vol. 5739 (Ed: W. Y. Yao, S. A. Stockman, F. E. Schubert), SPIE, Bellingham, WA **2005**.
[8] K. E. Chittibabu, R. Gaudiana, *US Patent 6 913 713*, **2005**.
[9] E. Cole, *US Patent 5 437 736*, **1995**.
[10] A. Duggal, L. Levinson, *US Patent 6 538 375*, **2003**.
[11] S. R. Forrest, *Chem. Rev.* **1997**, *97*, 1793.
[12] M. Shtein, H. F. Gossenberger, J. B. Benziger, S. R. Forrest, *J. Appl. Phys.* **2001**, *89*, 1470.
[13] C. W. Tang, S. A. Vanslyke, *Appl. Phys. Lett.* **1987**, *51*, 913.
[14] M. A. Baldo, S. R. Forrest, *Phys. Rev. B* **2001**, *64*, 085201.
[15] P. E. Burrows, Z. Shen, V. Bulovic, D. M. McCarty, S. R. Forrest, J. A. Cronin, M. E. Thompson, *J. Appl. Phys.* **1996**, *79*, 7991.
[16] V. Bulovic, V. B. Khalfin, G. Gu, P. E. Burrows, D. Z. Garbuzov, S. R. Forrest, *Phys. Rev. B* **1998**, *58*, 3730.
[17] P. T. Worthing, R. M. Amos, W. L. Barnes, *Phys. Rev. A* **1999**, *59*, 865.
[18] J. A. E. Wasey, W. L. Barnes, *J. Mod. Opt.* **2000**, *47*, 725.
[19] S. R. Forrest, D. D. C. Bradley, M. E. Thompson, *Adv. Mater.* **2003**, *15*, 1043.

  

[20] B. O'Connor, K. H. An, K. P. Pipe, Y. Zhao, M. Shtein, *Appl. Phys. Lett.* **2006**, *89*, 233 502.
[21] K. Yamashita, T. Mori, T. Mizutani, *J. Phys. D* **2001**, *34*, 740.
[22] A. P. Ghosh, L. J. Gerenser, C. M. Jarman, J. E. Fornalik, *Appl. Phys. Lett.* **2005**, *86*.
[23] S. H. Choi, Y. H. Park, C. J. Lee, D. G. Moon, J. Kang, M. H. Oh, G. K. Chang, J. I. Han, *Jpn. J. Appl. Phys.* Part 2 **2007**, *46*, 810.
[24] A. B. Chwang, M. A. Rothman, S. Y. Mao, R. H. Hewitt, M. S. Weaver, J. A. Silvernail, K. Rajan, M. Hack, J. J. Brown, X. Chu, L. Moro, T. Krajewski, N. Rutherford, *Appl. Phys. Lett.* **2003**, *83*, 413.
[25] P. E. Burrows, G. L. Graff, M. E. Gross, P. M. Martin, M. K. Shi, M. Hall, E. Mast, C. Bonham, W. Bennett, M. B. Sullivan, *Displays* **2001**, *22*, 65.
[26] M. H. Lu, J. C. Sturm, *J. Appl. Phys.* **2002**, *91*, 595.
[27] H. Riel, S. Karg, T. Beierlein, W. Riess, K. Neyts, *J. Appl. Phys.* **2003**, *94*, 5290.
[28] H. Riel, S. Karg, T. Beierlein, B. Ruhstaller, W. Riess, *Appl. Phys. Lett.* **2003**, *82*, 466.
[29] C. H. Cheung, A. B. Djurisic, C. Y. Kwong, H. L. Tam, K. W. Cheah, Z. T. Liu, W. K. Chan, P. C. Chui, J. Chan, A. D. Rakic, *Appl. Phys. Lett.* **2004**, *85*, 2944.
[30] C. H. Cheung, A. B. Djurisic, C. Y. Kwong, H. L. Tam, K. W. Cheah, Z. T. Liu, W. K. Chan, P. C. Chui, J. Chan, A. D. Rakic, *Opt. Commun.* **2005**, *248*, 287.
[31] C. F. Qiu, H. J. Peng, H. Y. Chen, Z. L. Xie, M. Wong, H. S. Kwok, *IEEE Trans. Electron Devices* **2004**, *51*, 1207.
[32] K. Neyts, P. De Visschere, D. K. Fork, G. B. Anderson, *J. Opt. Soc. Am. B* **2000**, *17*, 114.
[33] K. A. Neyts, *J. Opt. Soc. Am. A* **1998**, *15*, 962.
[34] K. Neyts, *Appl. Surf. Sci.* **2005**, *244*, 517.
[35] J. M. Lupton, B. J. Matterson, I. D. W. Samuel, M. J. Jory, W. L. Barnes, *Appl. Phys. Lett.* **2000**, *77*, 3340.
[36] K. H. An, B. O'Connor, K. P. Pipe, Y. Y. Zhao, M. Shtein, *Appl. Phys. Lett.* **2006**, *89*, 111 117.
[37] H. Kanno, Y. Sun, S. R. Forrest, *Appl. Phys. Lett.* **2005**, *86*, 263 502.
[38] M. Shtein, P. Peumans, J. B. Benziger, S. R. Forrest, *J. Appl. Phys.* **2003**, *93*, 4005.
[39] J. Rhee, H. H. Lee, *Appl. Phys. Lett.* **2002**, *81*, 4165.


  